Improving Leaf Area Index Retrieval Over Heterogeneous Surface by Integrating Textural and Contextual Information: A Case Study in the Heihe River Basin

Gaofei Yin, Jing Li, Qinhuo Liu, Longhui Li, Yelu Zeng, Baodong Xu, Le Yang, and Jing Zhao

***Abstract*—Spatial heterogeneity of land surface induces scaling bias in leaf area index (LAI) products. In optical remote sensing of vegetation, spatial heterogeneity arises both by textural and contextual effects. A case study made in the middle reach of the Heihe River Basin shows that the scaling bias in LAI retrieval is large up to 26% if the spatial heterogeneity within low-resolution pixels is ignored. To reduce the influence of spatial heterogeneity on LAI products, a correcting method combining both textural and contextual information is adopted, and the scaling bias may decrease to less than 2% in producing resolution-invariant LAI products.**

***Index Terms*—Land surface, remote sensing, spatial resolution, surface structures, surface texture, vegetation.**

I. Introduction

LEAF area index (LAI) influences vegetation photosynthesis, transpiration, and energy balance of the land surface [1]. It is a key parameter in climate, hydrology, and ecosystem productivity models [2]. Over the last decade, a number of LAI products became available. Most of them were derived from low resolution (refer to lower than or equal to 1 km in this letter) remote sensing measurements [3], [4]. When retrieving LAI products, a transfer relationship, such as look-up table [3], empirical relationship [4], and neural network [5], is required to relate remote sensing measurements to LAI. Generally, the transfer relationship is established and calibrated at patch scale and works well as long as the terrestrial surface is homogeneous [6]. However, in reality, the terrestrial surface within the footprint of a low-resolution pixel is almost heterogeneous [7]. When applied at pixel scale directly, the transfer relationship may induce scaling bias due to its nonlinearity and surface heterogeneity. Furthermore, scaling bias would propagate to the subsequent applications [8]. Therefore, it is necessary to take the spatial heterogeneity into account in estimating LAI from low-resolution satellite measurements.

In optical remote sensing of vegetation, surface heterogeneity arises both by textural (e.g., spatial clumping of foliage and growing difference) and contextual effects (e.g., the presence of multiple types of land cover) [9], [10]. Several methods for eliminating the influence of spatial heterogeneity on LAI retrieval have been developed. However, textural [11], [12] and contextual [9], [13] effects were taken into account separately in most of the existing scaling algorithms, so the residual scaling bias is retained for the low-resolution pixels with textural and contextual effects integrated together. Recently, Wu *et al.* [14] have developed a joint algorithm to eliminate both the textural and contextual effects. To evaluate the algorithm, they applied it to a simulated image constructed from a classification map other than in any practical remote sensing scenario. For the contextual effect, only the mixture of different vegetation types was accounted for in the evaluation.

Taking the middle reach of the Heihe River Basin in Northwest China as a study area, we have analyzed the relationship between scaling bias and heterogeneity. To reduce the scaling bias in LAI products, Wu's algorithm [14] is improved to account for the mixture of vegetation and nonvegetation, which is a more common scenario in our study area. Finally, the improved joint algorithm is evaluated against a Landsat5/TM image that covered the study area.

II. Methodology

A. Description of Spatial Heterogeneity

In this letter, spatial heterogeneity is described in terms of the following two components [15]:

1) the *density change* in the biophysical parameters within a patch;

Manuscript received January 29, 2014; revised May 16, 2014 and July 3, 2014; accepted July 14, 2014. This work was supported by the Action Plan of Western Development of the Chinese Academy of Sciences (No. KZCX2-XB3-15-2), the National Basic Research Program of China (No. 2013CB733401), the National Natural Science Foundation of China (No. 41271366), and the National High Technology Research and Development Program of China (No. 2012AA12A304 and 2012AA12A305).

G. Yin, Y. Zeng, and B. Xu are with the State Key Laboratory of Remote Sensing Science, Institute of Remote Sensing and Digital Earth, Chinese Academy of Sciences, Beijing 100101, China, and also with the University of Chinese Academy of Sciences, Beijing 100049, China.

J. Li is with the State Key Laboratory of Remote Sensing Science, Institute of Remote Sensing and Digital Earth, Chinese Academy of Sciences, Beijing 100101, China, and also with the Plant Functional Biology and Climate Change Cluster, University of Technology, Sydney, Ultimo, NSW 2007, Australia (e-mail: lijing01@radi.ac.cn).

Q. Liu, L. Yang, and J. Zhao are with the State Key Laboratory of Remote Sensing Science, Institute of Remote Sensing and Digital Earth, Chinese Academy of Sciences, Beijing 100101, China (e-mail: liuqh@radi.ac.cn).

L. Li is with the Plant Functional Biology and Climate Change Cluster, University of Technology, Sydney, Ultimo, NSW 2007, Australia.

Color versions of one or more of the figures in this paper are available online at http://ieeexplore.ieee.org.

Digital Object Identifier 10.1109/LGRS.2014.2341925

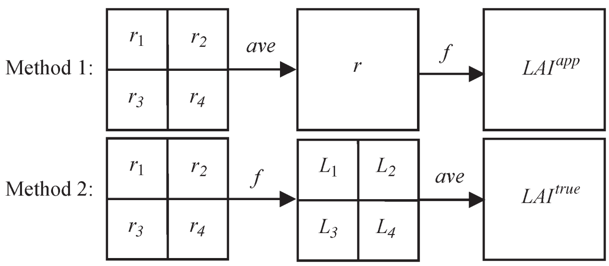

Fig. 1. Schematic representation of true LAI and apparent LAI calculations for one coarse pixel. r_i is the ith remote sensing measurement of the high-resolution pixel covered in a coarse pixel, and r is the averaged remote sensing measurement at the low resolution. L_i is the retrieved LAI from r_i. f and ave stand for transfer relationship and average, respectively.

2) the *mixture* of different land cover types within a low-resolution pixel, i.e., mixed pixel.

In a vegetation-dominant low-resolution pixel, the density change generally comes from foliage clumping and different growing conditions. It can be characterized by local variance [16], s^2, computed from the corresponding subpixels. Meanwhile, the land cover mixture can be quantified by vegetation area fraction a_v. The vegetation area fraction can serve as an indicator of the purity of a low-resolution pixel. The pixels with $a_v > 0.9$ are considered as pure pixels in this study. In a pure pixel, it is assumed that the heterogeneity comes from density change only. The local variance s^2 and vegetation area fraction a_v represent the textural and contextual effects, respectively.

B. Algorithms for Spatial Scaling

For a low-resolution pixel, its corresponding LAI value can be derived from low-resolution pixel directly (method 1) or arithmetic averaging of LAI values estimated by corresponding fine-resolution measurements (method 2; Fig. 1). Most of the radiative transfer models and LAI inversion algorithms are developed based on pure pixel. The LAI retrieved at fine resolution has high accuracy because the pixel is unmixed and there is no bias due to the scaling effects. Therefore, the result from method 2 is generally treated as the true LAI ($\mathrm{LAI}^{\mathrm{true}}$) [17]. Meanwhile, the obtained LAI from the former method is hereafter referred to be apparent LAI ($\mathrm{LAI}^{\mathrm{app}}$). The difference between $\mathrm{LAI}^{\mathrm{app}}$ and $\mathrm{LAI}^{\mathrm{true}}$ is defined as scaling bias [12], [17]

$$e_m = \mathrm{LAI}^{\mathrm{app}} - \mathrm{LAI}^{\mathrm{true}}. \tag{1}$$

The scaling bias is derived from the discrepancy of the representative space between low- and high-resolution pixels. Therefore, scaling bias can be seen as the representativeness error [18] of a low-resolution pixel.

To quantify the scaling bias at a given spatial resolution m, we introduce the mean relative scaling bias

$$e_m^{\mathrm{rel}} = \frac{1}{N}\sum_{i=1}^{N}\frac{\left|\mathrm{LAI}_i^{\mathrm{app}} - \mathrm{LAI}_i^{\mathrm{true}}\right|}{\mathrm{LAI}_i^{\mathrm{true}}} \tag{2}$$

where N is the number of low-resolution pixels covering the scene. $\mathrm{LAI}_i^{\mathrm{true}}$ and $\mathrm{LAI}_i^{\mathrm{app}}$ are the ith derived LAI values of the image using the first and second methods, respectively.

Within a pure pixel ($a_v > 0.9$), the remote sensing measurement values of subpixels vary continuously. The scaling bias e_m caused by the textural effect can be approximated by a second-order Taylor expansion, and the LAI with textural correction ($\mathrm{LAI}_{\mathrm{tex}}^{\mathrm{corr}}$) can be represented as [11], [12]

$$\mathrm{LAI}_{\mathrm{tex}}^{\mathrm{corr}} = \mathrm{LAI}^{\mathrm{app}} + f''(r_m)s_m^2/2 \tag{3}$$

where s_m^2 is the local variance, r_m is the aggregated remote sensing measurement at the low resolution m, and $f''(r_m)$ is the second derivative of the transfer relationship at r_m.

For the pixels mixed with different land covers, assuming that the subpixels in a low-resolution pixel are classified into vegetation and nonvegetation, the corrected LAI $\mathrm{LAI}_{\mathrm{con}}^{\mathrm{corr}}$ after removing the contextual effect can be calculated as [9]

$$\mathrm{LAI}_{\mathrm{con}}^{\mathrm{corr}} = a_v \mathrm{LAI}_{\mathrm{veg}} = a_v f(r_v) \tag{4}$$

where $\mathrm{LAI}_{\mathrm{veg}}$ is the LAI of the vegetation subpixels and r_v is the averaged remote sensing measurements over the vegetation subpixels within a low-resolution pixel.

In order to correct the textural effect in the vegetation subpixels, (3) is substituted into (4), and this yields

$$\mathrm{LAI}_{\mathrm{tex+con}}^{\mathrm{corr}} = a_v\left(f(r_v) + f''(r_v)s_v^2/2\right) \tag{5}$$

where s_v^2 is the local variance within the fraction of vegetation. $\mathrm{LAI}_{\mathrm{tex-con}}^{\mathrm{corr}}$ is the corrected LAI after removing the textural and contextual effects.

It is shown from (5) that the scaling bias is derived from the nonlinearity of the transfer relationship and the spatial heterogeneity of the land surface. The nonlinearity of f is quantified by its second derivative, and the spatial heterogeneity is quantified by vegetation area fraction and local variance within the vegetation region of the low-resolution pixel. Unlike [14] which placed emphasis on the mixture of different vegetation types, in this letter, we take into account a more common scenario in our study area (see Section III), namely, the mixture of vegetation and nonvegetation. To achieve this goal, the linear spectral unmixing technique is used to remove the influence of nonvegetation on the total reflectance of low-resolution pixels and get r_v in (5). In the spectral unmixing process, the reflectance of a low-resolution pixel is regarded as the sum of reflectances of vegetation and nonvegetation weighted by their respective area fractions. For simplicity, the reflectance of nonvegetation is assumed as constant in the study area.

III. Study Area and the LAI Transfer Relationship

The study area is in the middle reach of the Heihe River Basin in Zhangye city, Gansu, China (Fig. 2), which is located between 97.1° E–102.0° E and 37.7° N–42.7° N. The dominant land cover types in this area are crop, desert, and town. The Heihe Watershed Allied Telemetry Experimental Research program (HiWATER) [20] has been implemented in this basin since 2012. The highlights of this program are the use of some new observing techniques to capture multiscale heterogeneities and to address complex problems, such as heterogeneity, scaling, and uncertainty at the watershed scale. This research is

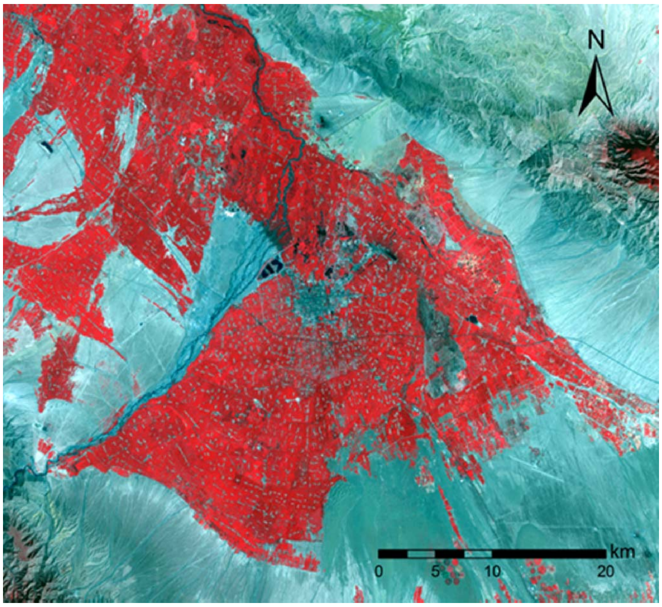

Fig. 2. TM image acquired on August 14, 2010, of the study area. The RGB components are channels 4 (0.76–0.96 μm), 3 (0.62–0.69 μm), and 2 (0.52–0.60 μm).

a part of the HiWATER to analyze and correct the influence of spatial heterogeneity on LAI retrieval. It is a fundamental work for the further research on the influence of the spatial heterogeneity on the energy balance, evapotranspiration estimation, etc.

A Landsat5/TM image acquired on August 14, 2010, with 1925 $\times$ 1700 pixels, as shown in Fig. 2, was used. The radiance calibration and atmospheric correction was implemented using FLAASH modal of ENVI software. The NDVI was calculated based on the corrected image. The histogram of the NDVI image shows a bimodal distribution, with the peaks located around 0.64 and 0.09 representing vegetation and nonvegetation, respectively. According to the NDVI threshold (0.15), the TM pixels were categorized into two types, namely, vegetation and nonvegetation. The obtained binary image was used to estimate the vegetation area fraction in aggregated low-resolution pixels. To calculate the reflectance of the subpixels of vegetation [r_v in (4) and (5)] in a low-resolution pixel through linear spectral unmixing technique, the reflectance values of nonvegetation (mainly soil) were set to be 0.19 and 0.25 at red and near-infrared bands based on the field measurement by the Analytical Spectral Devices [21].

The transfer relationship was constructed based on the SAILH model [22] simulation. The input parameters were set at typical values (see Table I). The spectral response function of the Landsat sensor was taken into account. Finally, the transfer relationship can be expressed by the following equation:

$$\mathrm{LAI} = 4.94\mathrm{NDVI}^{2.26}. \quad (6)$$

The transfer relationship (6) was used specifically to study the relative scaling bias at low resolution, and its accuracy to estimate the absolute LAI value does not influence the analysis results, so the validation of the transfer relationship was not addressed here. The formula for spatial bias correction in our study area can be deduced by substituting (6) into (5), i.e.,

$$\mathrm{LAI}^{\mathrm{corr}}_{\mathrm{tex+con}} = a_v \left(4.94\mathrm{NDVI}_v^{2.26} + 7.03\mathrm{NDVI}_v^{0.26} s^2_{\mathrm{NDVI}}\right) \quad (7)$$

where NDVI_v and s^2_{NDVI} are the NDVI and local variance of NDVI within the vegetation fraction.

In order to analyze the influence of spatial heterogeneity on the accuracy of LAI retrieval, two LAI images with 3000-m resolution were produced according to the two methods depicted in Fig. 1. According to method 1, the TM image after the preprocessing was first averaged to get the 3000-m reflectance image, and then, the apparent LAI was calculated based on (6). As to the true LAI, the LAI image was first calculated and then aggregated to 3000-m resolution.

IV. Results and Analysis

A. Scaling Bias Due to Spatial Heterogeneity

It is evident that the information on surface heterogeneity within a low-resolution pixel is mostly lost. This information-loss phenomenon reduces the accuracy of low-resolution LAI products. Fig. 3(a) shows a pixel-by-pixel comparison between $\mathrm{LAI}^{\mathrm{app}}$ and $\mathrm{LAI}^{\mathrm{true}}$ at 3000-m spatial resolution. It can be seen that $\mathrm{LAI}^{\mathrm{app}}$ is always less than $\mathrm{LAI}^{\mathrm{true}}$, i.e., the LAI is underestimated when retrieved from low-resolution image directly. There are many factors to cause the LAI underestimation of low-resolution pixels. Fig. 3(b)–(d) shows the difference between $\mathrm{LAI}^{\mathrm{app}}$ and $\mathrm{LAI}^{\mathrm{true}}$ when the vegetation area fractions inside the pixel lie in the range of (0.9, 1], (0.7, 0.9], and (0.5, 0.7], respectively. When the pixel is approximately pure as shown in Fig. 3(b), the relative scaling bias is 11%. The slight underestimation is mainly attributed to the convex of the transfer relationship between LAI and NDVI. According to Jensen's inequality, the convex transformation of a mean is less than or equal to the mean after convex transformation. When the pixel becomes more mixed with soil or desert as shown in Fig. 3(c) and (d), the relative scaling bias increases to 24% and 45%.

The relative scaling bias was mapped as shown in Fig. 4. Fig. 5 shows the corresponding vegetation purity map. The vegetation purity is defined as the vegetation area fraction in the whole pixel. The vegetation area fraction is generated based on the TM image by the NDVI threshold method. It can be seen from Figs. 4 and 5 that the spatial distribution patterns of the scaling bias and the vegetation purity are very similar. The large scaling biases are mainly distributed in the landscape transitional zones, e.g., urban–rural fringe and oasis–desert fringe. In the middle of the oasis, the relative scaling bias is generally lower than 20%. On the margin of the oasis, the relative scaling bias of a lot of pixels reaches higher than 40%. It reveals that the land cover mixture is a very important factor to be considered in the spatial scaling of LAI.

B. Results After Correction

Fig. 6 compares the true and apparent LAIs after scaling bias correction using different methods at 3000-m spatial resolution. We can see that the mean relative scaling bias decreases from

TABLE I
SAILH MODEL INPUT USED IN THE SIMULATION

Input	Leaf reflectance & transmitance	Leaf angle inclination	Hot spot index	Soil reflectance
Source	From LOPEX 93 database [19]	Spherical	0.01	From field measurement by ASD spectrometer

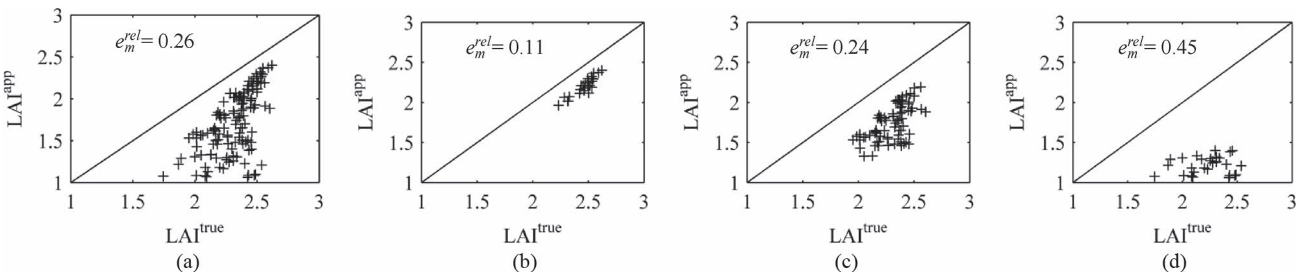

Fig. 3. Pixel-by-pixel comparison of LAI$^{\rm app}$ and LAI$^{\rm true}$ at 3000-m resolution. LAI$^{\rm true}$ is the true LAI value, and LAI$^{\rm app}$ is the apparent LAI value for (a) all vegetated pixels or pixels with vegetation area fraction within (b) (0.9, 1], (c) (0.7, 0.9], and (d) (0.5, 0.7].

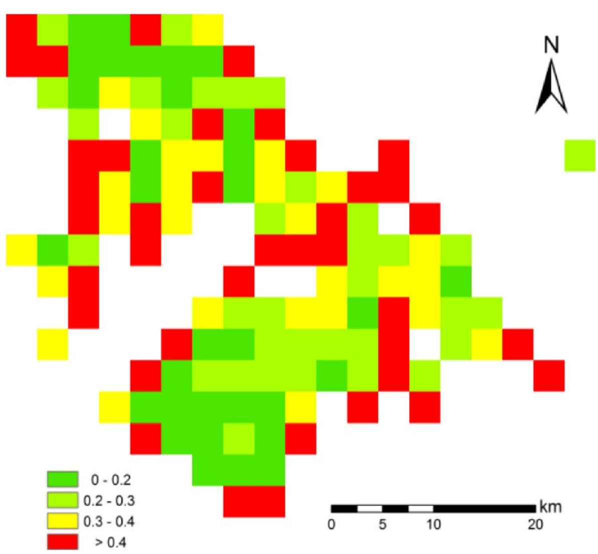

Fig. 4. Relative scaling bias map of LAI products at 3000-m resolution.

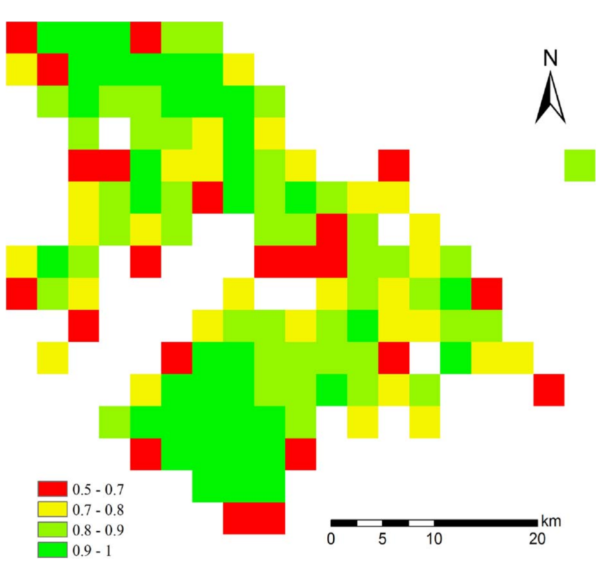

Fig. 5. Purity map of the study area at 3000-m resolution.

26% to 17% after correcting by texture and to 11% by context. It shows that the accuracy after the contextual correction is superior to that after the textural correction. This is determined by the heterogeneous characteristic of the study area. It is a crop planting area, and the crop growth in each patch is relatively homogeneous. The average subpixel scale local variance of NDVI in the vegetation area in all of the 3-km pixels is only 0.03. It reveals that no obvious heterogeneity in texture scale exists and, as a result, brings the limited scaling bias. However, the average vegetation fraction of the pixels tagged as vegetation in the study area is about 0.80. The nonvegetation types are mainly soil and desert. The mixture of the vegetation and nonvegetation is the main heterogeneity source. Therefore, the scaling correction by context improves the LAI inversion obviously. Promisingly, a noticeable improvement is obtained through the joint method. This joint method reduces the mean relative spatial scaling bias to 2%. The correlation between LAI$^{\rm corr}$ and LAI$^{\rm true}$ is also significantly improved as illustrated by the determination coefficient increasing from around 0.50 (corrected by either texture or context) to 0.80 (corrected by both texture and context).

The overall performances of the correction methods by either texture or context and both are illustrated in Fig. 7. The mean relative scaling bias increases with the decrease in the spatial resolution. The joint method gets resolution-invariant results with mean relative scaling bias always lower than 2%. This demonstrates the feasibility of the improved joint scaling method in our study area.

V. CONCLUSION

Taking the middle reach of the Heihe River Basin in Northwest China as a study area, the factors inducing scaling bias were quantitatively analyzed. The analysis results show that, without regard to the heterogeneity within low-resolution pixels, the LAI tends to be underestimated, and the mean relative scaling bias can be up to 26% at 3000-m resolution. The nonlinearity of the transfer relationship and the spatial heterogeneity in terms of textural and contextual effects account for the scaling bias. To reduce the influence of spatial heterogeneity

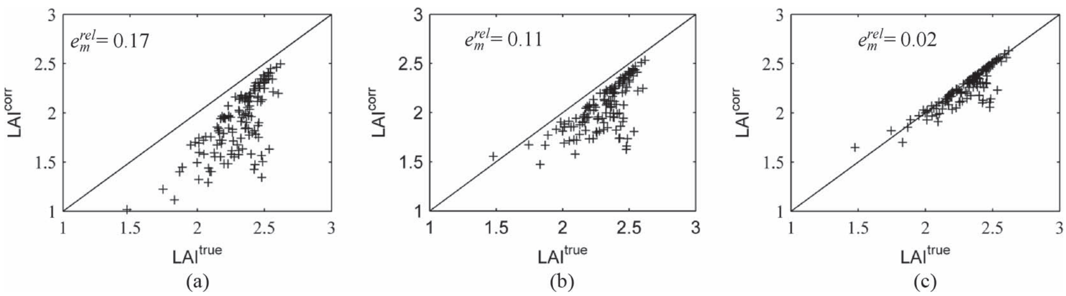

Fig. 6. Pixel-by-pixel comparison of LAI$^{\mathrm{corr}}$ and LAI$^{\mathrm{true}}$ at 3000-m resolution. LAI$^{\mathrm{true}}$ is the true LAI value, and LAI$^{\mathrm{corr}}$ is the apparent LAI value after correction by (a) texture, (b) context, or (c) both texture and context.

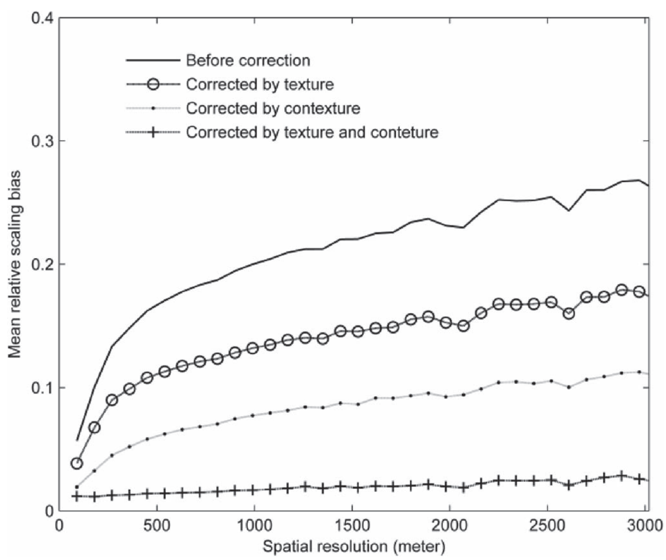

Fig. 7. Mean relative bias before and after correction as a function of spatial resolution.

on LAI retrieval, a correcting method combining both textural and contextual information is adopted. This method accounts for the density change in LAI within a patch and the mixture of vegetation and nonvegetation. Through this method, we got a resolution-invariant LAI product with scaling bias lower than 2% in the study area.

Due to the algorithm limitation, the physical mechanism of the influence of the spatial heterogeneity on LAI retrieval cannot be analyzed and discussed. Further understanding on the mechanism requires research and modeling on the radiative transfer process in the heterogeneous pixels, and it will be the focus of our future work.

ACKNOWLEDGMENT

The authors would like to thank Prof. S. Liu of Beijing Normal University, Beijing, China, and the anonymous reviewers for their insightful comments on this letter.

REFERENCES

[1] G. B. Bonan, "Land–atmosphere interactions for climate system models: Coupling biophysical, biogeochemical, ecosystem dynamical processes," *Remote Sens. Environ.*, vol. 51, no. 1, pp. 57–73, Jan. 1995.

[2] P. J. Sellers *et al.*, "Modeling the exchanges of energy, water, carbon between continents and the atmosphere," *Science*, vol. 275, no. 5299, pp. 502–509, Jan. 1997.

[3] R. B. Myneni *et al.*, "Global products of vegetation leaf area and fraction absorbed PAR from year one of MODIS data," *Remote Sens. Environ.*, vol. 83, no. 1/2, pp. 214–231, Nov. 2002.

[4] F. Deng, J. M. Chen, S. Plummer, M. Z. Chen, and J. Pisek, "Algorithm for global leaf area index retrieval using satellite imagery," *IEEE Trans. Geosci. Remote Sens.*, vol. 44, no. 8, pp. 2219–2229, Aug. 2006.

[5] F. Baret *et al.*, "GEOV1: LAI and FAPAR essential climate variables and FCOVER global time series capitalizing over existing products. Part 1: Principles of development and production," *Remote Sens. Environ.*, vol. 137, pp. 299–309, Oct. 2013.

[6] F. Baret *et al.*, "Evaluation of the representativeness of networks of sites for the global validation and intercomparison of land biophysical products: Proposition of the CEOS-BELMANIP," *IEEE Trans. Geosci. Remote Sens.*, vol. 44, no. 7, pp. 1794–1803, Jul. 2006.

[7] X. Li *et al.*, "Watershed allied telemetry experimental research," *J. Geophy. Res.*, vol. 114, no. D22, pp. D22103-1–D22103-19, Nov. 2009.

[8] M. El Maayar and J. M. Chen, "Spatial scaling of evapotranspiration as affected by heterogeneities in vegetation, topography, soil texture," *Remote Sens. Environ.*, vol. 102, no. 1/2, pp. 33–51, May 30, 2006.

[9] J. M. Chen, "Spatial scaling of a remotely sensed surface parameter by contexture," *Remote Sens. Environ.*, vol. 69, no. 1, pp. 30–42, Jul. 1999.

[10] N. Widen, "Assessing the accuracy of land surface characteristics estimated from multi-angular remotely sensed data," *Int. J. Remote Sens.*, vol. 25, no. 6, pp. 1105–1117, Mar. 2004.

[11] Z. Hu and S. Islam, "A framework for analyzing and designing scale invariant remote sensing algorithms," *IEEE Trans. Geosci. Remote Sens.*, vol. 35, no. 3, pp. 747–755, May 1997.

[12] S. Garrigues, D. Allard, F. Baret, and M. Weiss, "Influence of landscape spatial heterogeneity on the non-linear estimation of leaf area index from moderate spatial resolution remote sensing data," *Remote Sens. Environ.*, vol. 105, no. 4, pp. 286–298, Dec. 30, 2006.

[13] J. M. Chen, X. Chen, and W. Ju, "Effects of vegetation heterogeneity and surface topography on spatial scaling of net primary productivity," *Biogeosciences*, vol. 10, no. 7, pp. 4879–4896, Jul. 2013.

[14] H. Wu, B. H. Tang, and Z. L. Li, "Impact of nonlinearity and discontinuity on the spatial scaling effects of the leaf area index retrieved from remotely sensed data," *Int. J. Remote Sens.*, vol. 34, no. 9/10, pp. 3503–3519, May 2013.

[15] S. Garrigues, D. Allard, F. Baret, and M. Weiss, "Quantifying spatial heterogeneity at the landscape scale using variograrn models," *Remote Sens. Environ.*, vol. 103, no. 1, pp. 81–96, Jul. 2006.

[16] C. E. Woodcock and A. H. Strahler, "The factor of scale in remote sensing," *Remote Sens. Environ.*, vol. 21, no. 3, pp. 311–332, Apr. 1987.

[17] Y. H. Tian *et al.*, "Multiscale analysis and validation of the MODIS LAI product: I. Uncertainty assessment," *Remote Sens. Environ.*, vol. 83, no. 3, pp. 414–430, Dec. 2002.

[18] X. Li, "Characterization, controlling, reduction of uncertainties in the modeling and observation of land-surface systems," *Sci. Chin. Earth Sci.*, vol. 57, no. 1, pp. 80–87, Jan. 2013.

[19] B. Hosgood *et al.*, "Leaf Optical Properties EXperiment 93 (LOPEX93)," Eur. Commiss., Brussels, Belgium, 1995.

[20] X. Li *et al.*, "Heihe Watershed Allied Telemetry Experimental Research (HiWATER): Scientific objectives and experimental design," *Bull. Amer. Meteorol. Soc.*, vol. 94, no. 8, pp. 1145–1160, Aug. 2013.

[21] *FieldSpec Pro Users Guide*, Analytical Spectral Devices, Boulder, CO, USA, 2002.

[22] W. Verhoef, "Light-scattering by leaf layers with application to canopy reflectance modeling: The SAIL model," *Remote Sens. Environ.*, vol. 16, no. 2, pp. 125–141, Oct. 1984.